



## Magnetic Composite Coatings FeC and NiC Synthesized With Arabinogalactan

Sergey V. Stolyar<sup>1,2,3</sup> , Irina G. Vazhenina<sup>2</sup> , Roman N. Yaroslavtsev<sup>1,2</sup> , Lidia A. Chekanova<sup>2</sup>, Elena V. Cheremiskina<sup>1</sup>, and Yuri L. Mikhlin<sup>4</sup>

<sup>1</sup>Krasnoyarsk Scientific Center, Federal Research Center KSC SB RAS, 660036 Krasnoyarsk, Russia

<sup>2</sup>Kirensky Institute of Physics, Federal Research Center KSC SB RAS, 660036 Krasnoyarsk, Russia

<sup>3</sup>Siberian Federal University, 660041 Krasnoyarsk, Russia

<sup>4</sup>Institute of Chemistry and Chemical Technology, Federal Research Center KSC SB RAS, 660036 Krasnoyarsk, Russia

Received 7 Feb 2022, revised 20 Mar 2022, accepted 25 Mar 2022, published 4 Apr 2022, current version 28 Apr 2022.

**Abstract**—In this work, we investigated the ferromagnetic resonance spectra of metal/carbon composite coatings. FeC and NiC coatings were synthesized by electroless deposition using polysaccharide arabinogalactan. An analysis of the angular dependences of the resonance field showed that the coatings consist of three magnetic phases separated by a nonmagnetic phase of carbon.

**Index Terms**—Magnetism in solids, electroless deposition, magnetic coatings, ferromagnetic resonance.

### I. INTRODUCTION

A considerable interest in metal cover based on transition metals, for example, to absorb spread spectrum microwave radiation [Saib 2006, Wen 2006, Meng 2009, Liu 2010], stimulates development and research on not only new alloys but also the modernization of synthetic methods that already exist. Among the existing methods [Feng 2008, Vázquez 2009, Lv 2010, Moradi 2010, Brosseau 2011], electroless deposition is the simplest and most economical method for synthesizing metal coatings. Also, the advantages of this technique are the quality of the coating, physical and mechanical properties, and corrosion resistance [Agarwala 2003, Sudagar 2013]. The use of classical reducing agents [Domenech 2003, Cheong 2004, Yaroslavtsev 2014, Vazhenina 2017, Iskhakov 2020] has been accompanied by toxic chemical reagents, and therefore, an important line of research is the search for environmentally friendly reducing agents. The use of green chemistry approaches is promising, i.e., the use of plant extracts in the synthesis of nanomaterials. In this work, as a reducing agent, we used the polysaccharide arabinogalactan [Gasilova 2013, Komogortsev 2021], isolated from larch to prepare ferromagnetic metal coatings.

The proposed changes of chemical agent have influence on chemical features, structure, and magnetic properties of obtained coatings. To carry out an integrated study of both structure and magnetic features, the ferromagnetic resonance (FMR) method, which is the most informative and simple to analyze, was chosen.

In view of the above, the aim of this work was the preparation and study of chemical and magnetic structure of composite coatings based on Fe-C and Ni-C obtained by electroless deposition.

### II. MATERIALS AND METHODS

#### A. Sample Preparation

Ferromagnetic coatings were synthesized by electroless deposition using arabinogalactan. Deposition of Fe-C coatings was carried out

from an aqueous solution of the following composition: iron sulfate–30 g/l, sodium citrate–50 g/l, EDTA-Na2–20 g/l, arabinogalactan–10 g/l, NH<sub>4</sub>OH to reach 11 pH. Deposition of Ni-C coatings was carried out from an aqueous solution of the following composition: nickel sulfate–10 g/l, sodium citrate–10 g/l, arabinogalactan–10 g/l, NH<sub>4</sub>OH to reach 11 pH. The temperature of the solution was maintained with a thermostat at 85 °C.

The substrate was Cu foil, which was located into Al contact during the deposition process. The decomposition of arabinogalactan in an alkaline solution during the preparation of coatings was investigated according to the data obtained. With an increase in the duration of the process, the value of the average molecular weight decreases, and the curves of the molecular weight distribution shift to the low molecular weight region. We assume that during the process, alkaline hydrolysis of arabinogalactan molecules occurs. The thickness of coatings is 1 μm.

#### B. Structure and Elemental Composition

The coatings studied in this work are metal/carbon composites in which the metal phase is distributed in a carbon matrix. Elemental analysis performed by EDX spectroscopy showed that the coating contains ~20% carbon.

Fig. 1 shows X-ray diffraction patterns of samples: Ni-C and Fe-C coatings. The X-ray diffraction patterns contain both reflections corresponding to ferromagnetic metals and reflections corresponding to a copper substrate. Along with reflections from metal planes, low-intensity reflections were recorded at  $2\Theta = 27^\circ$ . This reflection is due to reflections from closely packed planes of the graphite phase. This indicates that carbon is deposited in the form of graphite.

The photoelectron spectra (see Fig. 2) were recorded with a SPECS spectrometer equipped with a PHOIBOS 150 MCD9 hemispherical energy analyzer using monochromatic Al K $\alpha$  radiation of the dual anode X-ray tube at the analyzer transmission energy of 20 eV for the survey spectra or 10 eV for narrow scans. Typical assignment of carbon lines with increasing bond energy is aliphatic carbon (285–285.5 eV), alcohol and ether groups (286–287 eV), ketone groups (287–288 eV),

Corresponding author: Roman N. Yaroslavtsev (e-mail: yar-man@bk.ru).

Digital Object Identifier 10.1109/LMAG.2022.3164631

1949-307X © 2022 IEEE. Personal use is permitted, but republication/redistribution requires IEEE permission.

See <https://www.ieee.org/publications/rights/index.html> for more information.

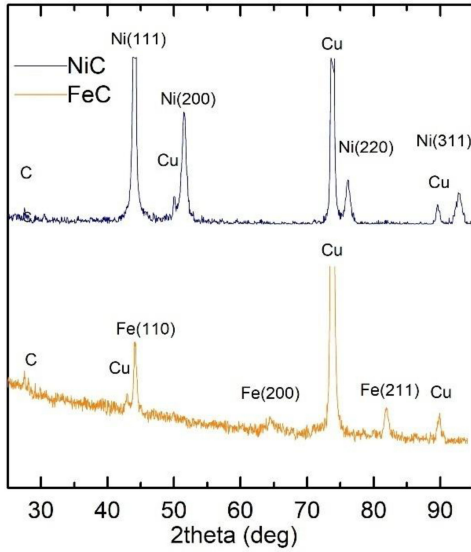


Fig. 1. X-ray diffraction patterns.

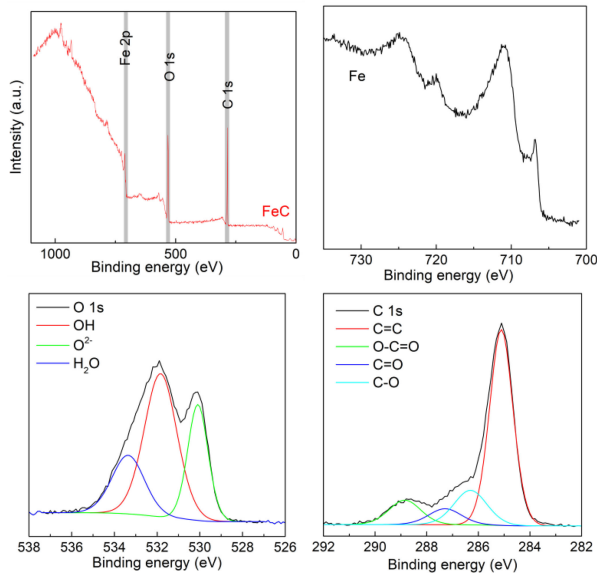


Fig. 2. X-ray photoelectron spectrum of Fe-C coating.

and carboxyl groups (289–290 eV), depending on protonation and bonds with the substrate. Oxygen lines of about 530 eV are  $O^{2-}$  in oxides, metal hydroxides, oxygen in functional groups of organic matter, and adsorbed water.

### C. Ferromagnetic Resonance

The microwave spectra of the films were obtained on the equipment of the Krasnoyarsk Regional Center of Research Equipment of Federal Research Center, Krasnoyarsk Science Center, Siberian Branch of the Russian Academy of Sciences (spectrometer ELEXSYS E580, Bruker, Germany). The microwave spectra were measured at room temperature in the X-band (resonator pumping frequency  $f = 9.2$  GHz); the sample was placed in the antinode of an alternating magnetic field  $\vec{h}$  of a cavity resonator. The measurements were carried out both when the

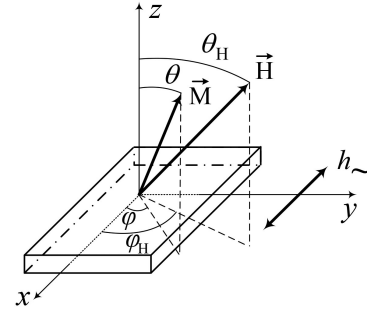


Fig. 3. Experiment geometry.

direction of the constant magnetic field  $\vec{H}$  was changed in the film plane (along the angle  $\varphi_H$ ) and in the plane parallel to the normal to the film (along the angle  $\theta_H$ ) (see Fig. 3).

The microwave absorption curves, which have a complex shape, were decomposed into components using the differentiated Lorentz function, the choice of which took into account the absence of the contribution of the electrical component (due to the design of the resonator and the size of the sample).

The general expression of the FMR resonance frequency  $\omega_0$  in the spherical coordinate system [Smit 1955, Suhl 1955, Artman 1957] in terms of the total energy of the magnetic system  $E$ , taking into account the Landau–Lifshitz equation for the motion of the magnetization  $M$ , given by the polar  $\theta$  and azimuthal  $\varphi$  angles, can be represented as

$$\omega_0 = \frac{\gamma}{M \sin \theta} \left[ \frac{\partial^2 E}{\partial \theta^2} \cdot \frac{\partial^2 E}{\partial \varphi^2} - \left( \frac{\partial^2 E}{\partial \theta \partial \varphi} \right)^2 \right]^{1/2} \quad (1)$$

where  $\gamma = 1.758 \cdot 10^7$  Hz/Oe—gyromagnetic ratio.

The equilibrium position of the magnetization vector is determined by the following relation:

$$\frac{\partial E}{\partial \varphi} = \frac{\partial E}{\partial \theta} = 0 \quad (2)$$

and the free energy density

$$\begin{aligned} E = & -M \cdot H [\sin(\theta) \cdot \sin(\theta_H) \cdot \cos(\varphi - \varphi_H) + \cos(\theta) \cdot \cos(\theta_H)] \\ & + \frac{K_1}{4} [\sin^4(\theta) \cdot \sin^2(2\varphi) + \sin^2(2\theta)] \\ & + \frac{K_2}{16} \cdot \sin^2(2\theta) \cdot \sin^2(\theta) \cdot \sin^2(2\varphi) \\ & + [2\pi M^2 + K_n] \cdot \cos^2(\theta) + K_u \cdot \sin^2(\theta) \cdot \sin^2(\varphi - \varphi_0) \end{aligned} \quad (3)$$

where  $\theta_H$  and  $\varphi_H$  are the polar and azimuthal angle of the external constant bias field  $H$ ;  $K_1$  and  $K_2$  are the first and second cubic anisotropy constants;  $K_n$  is the constant of perpendicular uniaxial anisotropy;  $K_u$  is the constant of uniaxial anisotropy in a plane acting at an angle  $\varphi_0$ .

The value of the resonant field  $H_0$  of the uniform mode for an arbitrary direction of the external magnetic field can be found by numerically solving the system of equations (1)–(3). Extreme cases for a magnetically isotropic sample in the form of an infinitely thin disk were obtained by [Kittel 1948]

$$\begin{aligned} \frac{\omega_0}{\gamma} &= (H_0 - 4\pi M) \quad (\text{at } \theta = \theta_H = 0^\circ) \\ \left( \frac{\omega_0}{\gamma} \right)^2 &= H_0 (H_0 + 4\pi M) \quad (\text{at } \theta = \theta_H = 90^\circ) \end{aligned} \quad (4)$$

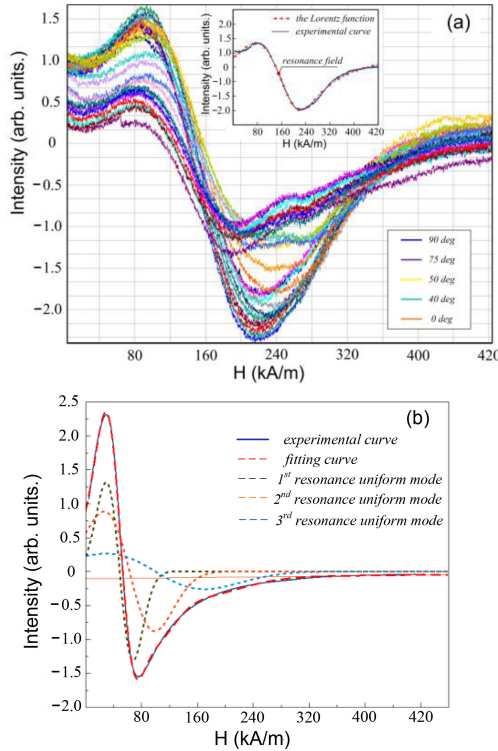


Fig. 4. (a) Ni-C coating spectra measured in the in-plane orientation in the full angular range ( $0 < \phi_H < 180$ ; the curves with different colors correspond to different angles of the applied magnetic field). The inset shows the experimental spectrum at  $\phi_H = 0^\circ$  and its fitting curve. (b) Example of a spectrum of an Fe-C coating (the field is applied along the plane,  $\phi_H = 0^\circ$  and  $\theta_H = 90^\circ$ ) and its decomposition into components.

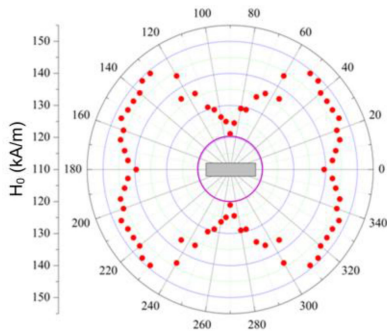


Fig. 5. In-plane polar plot of Ni-C coating.

where  $M$  is the saturation magnetization.

### III. RESULTS AND DISCUSSION

The synthesized coatings were investigated by the FMR method. The in-plane and out-of-plane angular dependences of resonance were investigated. Examples of FMR spectra are shown in Fig. 4.

The resonance absorption curves of the Ni-C coating [see Fig. 4(a)] have enough symmetric form, and each curve was considered as one mode characterized by resonance field  $H$ . The angular dependence of the FMR resonance field measured in the in-plane orientation of the Ni-C coating is shown in Fig. 5. The magenta line in the graph shows

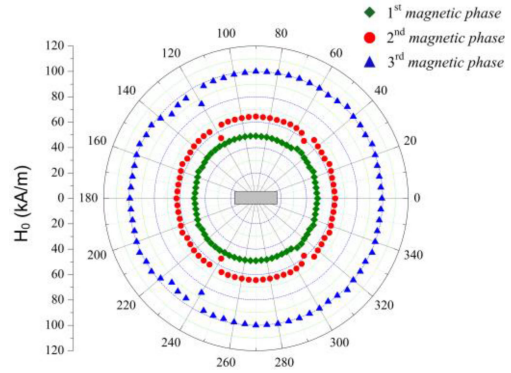


Fig. 6. In-plane polar plot of Fe-C coating.

the resonant field of an isotropic nickel film. As can be seen, the coating is rather anisotropic in the plane; the resonance field value varies from  $\sim 120$  to  $\sim 150$  kA/m. There are two axes of hard magnetization, located at an angle of  $80^\circ$  relative to each other.  $M$  can be found by (4) at  $\theta_H = 90^\circ$ , and its value is about 0.09 T.

The microwave spectra of the Fe-C coating have a complex shape, which cannot be compared with only one Lorentz function. The smallest number of Lorentz functions, the addition of which led to small deviations (no more than 5%) of the fitting curve from the experimental one, was three. Also, when choosing the number of individual functions involved in the fitting, we took into account that the parameters determined by the FMR method are integral. Based on this, the values of the estimated values have a qualitative character. Thus, the difference between the shape of the curve and the Lorentz function indicates the heterogeneity of the distribution of magnetic parameters over the coating volume. Each experimental curve was decomposed into three modes [see Fig. 4(b)].

The angular dependences of the resonance field of individual modes shown in Fig. 6 indicate that the Fe-C coating is magnetically isotropic in the plane. Therefore, the angular dependences of the resonance were measured in the out-of-plane orientation (see Fig. 7).

The measured resonance absorption curves have an asymmetric, non-Lorentzian shape; for their analysis, each spectrum was decomposed into three components using the Lorentz function [see Fig. 4(b)]. Fig. 7 shows the out-of-plane angular dependences of the resonance field, resonance line width, and intensity for three absorption lines. As the angle between the applied field and the film plane increases, the resonance field and the resonance line width increase while the intensity of resonance absorption decreases.

The presence of three resonance absorption lines tells us about the existence of three magnetic phases separated in space.

The united solution of (1)–(3) allowed us to define the value of the resonance field of each individual mode in the full range of  $\theta_H$ . The value of perpendicular anisotropy field  $H_{an} = 2K_n/M$  was a variable parameter.  $M$  was calculated from spectra in parallel geometry by (4).  $K_1$  and  $K_2$  are equal to zero due to the film, which is nanocrystalline. According to data in-plane measuring,  $K_u$  is equal to zero. The fitting result is the numeric value  $H_{an}$ , the accuracy of definition of which is about  $\sim 5$  kA/m. Fig. 8 shows the angular dependences of the FMR resonance field of three magnetic phases, as well as fitting curves.

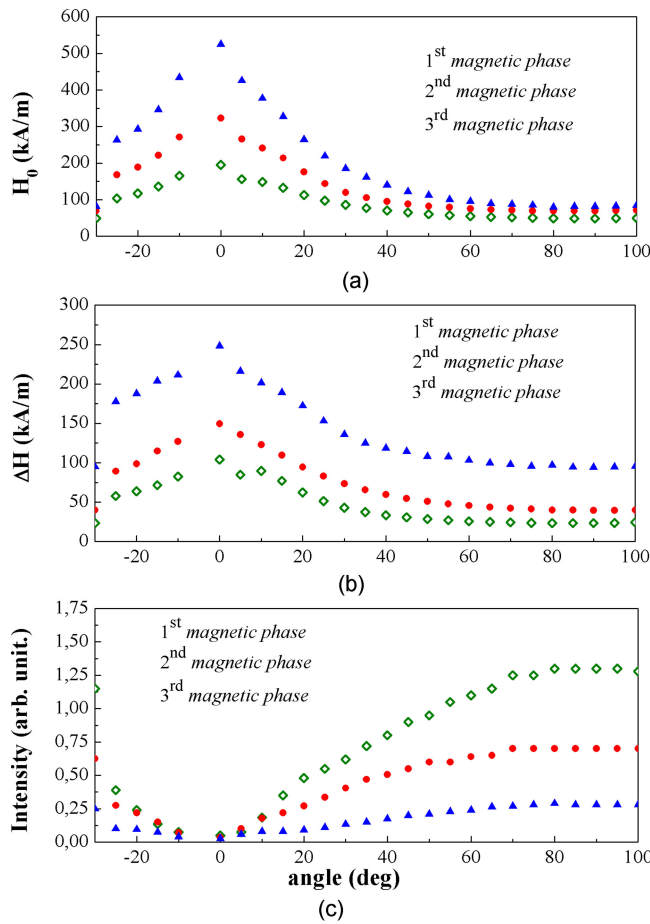


Fig. 7. (a) Out-of-plane angular dependences of the resonance field  $H_0$ , (b) resonance linewidth  $\Delta H$ , and (c) intensity for Fe-C coating.

TABLE 1. Magnetic parameters of Fe-C obtained from fitting.

	M, T	$H_{an}$ , kA/m
1 <sup>st</sup> magnetic phase	$(140 \pm 7) \cdot 10^{-3}$	$120 \pm 6$
2 <sup>nd</sup> magnetic phase	$(90 \pm 4.5) \cdot 10^{-3}$	$120 \pm 6$
3 <sup>rd</sup> magnetic phase	$(80 \pm 4) \cdot 10^{-3}$	$-63 \pm 3$

Table 1 shows the results of fitting the angular dependences of the three magnetic phases. The first magnetic phase with parameters  $M \approx 0.14$  T and  $H_{an} \approx 120$  kA/m corresponds to metallic Fe. A high positive value of the anisotropy field indicates that the easy axis of anisotropy is directly perpendicular to the plane of the film, i.e., predominantly perpendicular crystallite growth takes place. Such a coating formation was previously observed in electron microscopic images in films synthesized with arabinogalactan [Stolyar 2020].

The second magnetic phase with the parameters  $M \approx 0.09$  T and  $H_{an} \approx 120$  kA/m apparently corresponds to the metal phase with a reduced magnetization—the Fe-C solid solution, with the same crystallite orientation.

The third magnetic phase with the parameters  $M \approx 0.08$  T and  $H_{an} \approx -63$  kA/m corresponds to iron oxide with crystallites oriented along the film plane.

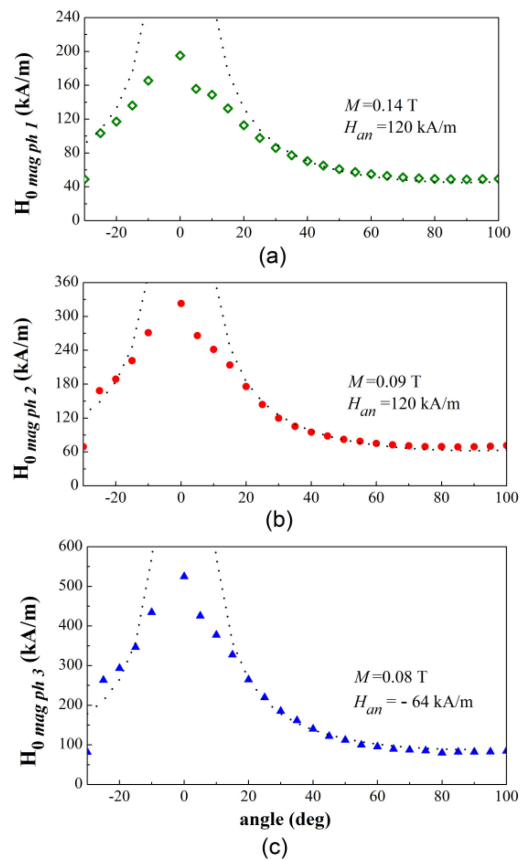


Fig. 8. Fitting curves for every magnetic phase (dashed line) and the angular dependences of the experimental resonance fields of FMR curves (rhombus, sphere, and triangle). (a) First magnetic phase. (b) Second magnetic phase. (c) Third magnetic phase.

Thus, composite coatings consist of three magnetic phases separated by a nonmagnetic carbon layer.

#### IV. CONCLUSION

The analysis of study results were carried out by FMR; the X-ray photoelectron method demonstrates that chosen synthesis method allows us to produce composite coating 3-D metal-carbon. Carbon exists in the form of graphite. Obtained coatings are composites in which the heterogeneous structure was found. The study demonstrates that the magnetic parameters of the coating (the type and magnitude of anisotropy, the presence or absence of areas with their own sets of magnetic characteristics) depend on the alloy. Thus, in-plane measurements by the FMR method allow us to define the presence of the biaxial anisotropy in the plane for Ni-C coating. At the same time, the Ni-C coating has a fairly uniform magnetization distribution over the thickness, the effective value of which is about 0.09 T. The results obtained by FMR for Fe-C coatings demonstrate the presence of three magnetic phases, each of which has its own value of effective magnetization and anisotropy. The angular dependences of the resonance field measured both in-plane and out-of-plane of the sample show the presence of only perpendicular magnetic anisotropy for each magnetic phase. It is possible that the difference in the type of anisotropy and the formation of regions having inhomogeneous magnetic parameters



is caused by the predominantly columnar growth of crystallites during the procedure, i.e., the texture of the coating. A more detailed study of the latter assumption will be the direction of our next research.

## ACKNOWLEDGMENT

This work was supported by Russian Foundation for Basic Research, Krasnoyarsk Territory and Krasnoyarsk Regional Fund of Science under Project 20-42-240010. The authors thank the Center of Collective Use of the Federal Research Center, Krasnoyarsk Science Center of the Siberian Branch of the Russian Academy of Sciences for the provided equipment.

## REFERENCES

- Agarwala R C, Agarwala V (2003), "Electroless alloy/composite coatings: A review," *Sadhana*, vol. 28, pp. 475–493, doi: [10.1007/BF02706445](https://doi.org/10.1007/BF02706445).
- Artman J O (1957), "Ferromagnetic resonance in metal single crystals," *Phys. Rev.*, vol. 105, pp. 74–84, doi: [10.1103/PhysRev.105.74](https://doi.org/10.1103/PhysRev.105.74).
- Brosseau C (2011), "Emerging technologies of plastic carbon nanoelectronics: A review," *Surf. Coatings Technol.*, vol. 206, pp. 753–758, doi: [10.1016/j.surfcoat.2011.02.017](https://doi.org/10.1016/j.surfcoat.2011.02.017).
- Cheong W J, Luan B L, Shoensmith D W (2004), "The effects of stabilizers on the bath stability of electroless Ni deposition and the deposit," *Appl. Surf. Sci.*, vol. 229, pp. 282–300, doi: [10.1016/j.apsusc.2004.02.003](https://doi.org/10.1016/j.apsusc.2004.02.003).
- Domenech S C, Lima E, Jr., Dragoc V, De Lima J C, Borges N G, Jr., Avila A O A, Soldi V (2003), "Electroless plating of nickel–phosphorous on surface-modified poly(ethylene terephthalate) films," *Appl. Surf. Sci.*, vol. 220, pp. 238–250, doi: [10.1016/S0169-4332\(03\)00815-8](https://doi.org/10.1016/S0169-4332(03)00815-8).
- Feng X, Liao G, Du J, Dong L, Jin K, Jian X (2008), "Electrical conductivity and microwave absorbing properties of nickel-coated multiwalled carbon nanotubes/poly(phthalazinone ether sulfone ketone)s composites," *Polym. Eng. Sci.*, vol. 48, pp. 1007–1014, doi: [10.1002/pen.21028](https://doi.org/10.1002/pen.21028).
- Gasilova E R, Matveeva G N, Aleksandrova G P, Sukhov B G, Trofimov B A (2013), "Colloidal aggregates of Pd nanoparticles supported by larch arabinogalactan," *J. Phys. Chem. B*, vol. 117, pp. 2134–2141, doi: [10.1021/jp3118242](https://doi.org/10.1021/jp3118242).
- Iskhakov R S, Stolyar S V, Chekanova L A, Vazhenina I G (2020), "Spin-wave resonance in one-dimensional magnonic crystals by an example of multilayer Co–P films," *Phys. Solid State*, vol. 62, pp. 1861–1867, doi: [10.1134/S1063783420100121](https://doi.org/10.1134/S1063783420100121).
- Kittel C (1948), "On the theory of ferromagnetic resonance absorption," *Phys. Rev.*, vol. 73, pp. 155–161, doi: [10.1103/PhysRev.73.155](https://doi.org/10.1103/PhysRev.73.155).
- Komogortsev S V, Stolyar S V, Chekanova L A, Yaroslavtsev R N, Bayukov O A, Velikanov D A, Volochaev M N, Eroshenko P E, Iskhakov R S (2021), "Square plate shaped magnetite nanocrystals," *J. Magn. Magn. Mater.*, vol. 527, pp. 167730, doi: [10.1016/j.jmmm.2021.167730](https://doi.org/10.1016/j.jmmm.2021.167730).
- Liu L, Duan Y, Ma L, Liu S, Yu Z (2010), "Microwave absorption properties of a wave-absorbing coating employing carbonyl-iron powder and carbon black," *Appl. Surf. Sci.*, vol. 257, pp. 842–846, doi: [10.1016/j.apsusc.2010.07.078](https://doi.org/10.1016/j.apsusc.2010.07.078).
- Lv R, Kang F, Gu J, Wang K, Wu D (2010), "Synthesis, field emission and microwave absorption of carbon nanotubes filled with ferromagnetic nanowires," *Sci. China Technol. Sci.*, vol. 53, pp. 1453–1459, doi: [10.1007/s11431-010-3145-y](https://doi.org/10.1007/s11431-010-3145-y).
- Meng W, Yuping D, Shunhua L, Xiaogang L, Zhijiang J (2009), "Absorption properties of carbonyl-iron/carbon black double-layer microwave absorbers," *J. Magn. Magn. Mater.*, vol. 321, pp. 3442–3446, doi: [10.1016/j.jmmm.2009.06.040](https://doi.org/10.1016/j.jmmm.2009.06.040).
- Moradi A (2010), "Microwave response of magnetized hydrogen plasma in carbon nanotubes: Multiple reflection effects," *Appl. Opt.*, vol. 49, pp. 1728, doi: [10.1364/AO.49.001728](https://doi.org/10.1364/AO.49.001728).
- Saib A, Bednarz L, Daussin R, Bailly C, Lou X, Thomassin J-M, Pagnoulle C, Detrembleur C, Jerome R, Huynen I (2006), "Carbon nanotube composites for broadband microwave absorbing materials," *IEEE Trans. Microw. Theory Techn.*, vol. 54, pp. 2745–2754, doi: [10.1109/TMTT.2006.874889](https://doi.org/10.1109/TMTT.2006.874889).
- Smit J, Beljers H G (1955), "Ferromagnetic resonance absorption in BaFe<sub>12</sub>O<sub>19</sub>, a highly anisotropic crystal," *Philips Res. Rep.*, vol. 10, pp. 113.
- Stolyar S V, Yaroslavtsev R N, Chekanova L A, Rautskii M V, Bayukov O A, Chermiskina E V, Nemtsev I V, Volochaev M N, Iskhakov R S (2020), "Ferromagnetic resonance in iron tubes deposited on a copper grid," *J. Magn. Magn. Mater.*, vol. 511, pp. 166979, doi: [10.1016/j.jmmm.2020.166979](https://doi.org/10.1016/j.jmmm.2020.166979).
- Sudagar J, Lian J, Sha W (2013), "Electroless nickel, alloy, composite and nano coatings—A critical review," *J. Alloys Compd.*, vol. 571, pp. 183–204, doi: [10.1016/j.jallcom.2013.03.107](https://doi.org/10.1016/j.jallcom.2013.03.107).
- Suhl H (1955), "Ferromagnetic resonance in nickel ferrite between one and two kilomegacycles," *Phys. Rev.*, vol. 97, pp. 555–557, doi: [10.1103/PhysRev.97.555.2](https://doi.org/10.1103/PhysRev.97.555.2).
- Vazhenina I G, Chekanova L A, Iskhakov R S (2017), "Spin–wave resonance as a way of studying the constant of surface anisotropy, using films of Fe–Ni alloy as an example," *Bull. Russian Acad. Sci. Phys.*, vol. 81, pp. 308–310, doi: [10.3103/S1062873817030388](https://doi.org/10.3103/S1062873817030388).
- Vázquez E, Prato M (2009), "Carbon nanotubes and microwaves: Interactions, responses, and applications," *ACS Nano*, vol. 3, pp. 3819–3824, doi: [10.1021/nn901604j](https://doi.org/10.1021/nn901604j).
- Wen B, Zhao J, Duan Y, Zhang X, Zhao Y, Dong C, Liu S, Li T (2006), "Electromagnetic wave absorption properties of carbon powder from catalysed carbon black in X and Ku bands," *J. Phys. D: Appl. Phys.*, vol. 39, pp. 1960–1962, doi: [10.1088/0022-3727/39/9/036](https://doi.org/10.1088/0022-3727/39/9/036).
- Yaroslavtsev R N, Chekanova L A, Komogortsev S V, Iskhakov R S (2014), "Effect of sodium hypophosphite content to the deposition rate, structure and magnetic properties of electroless deposited Ni–P alloy," *Solid State Phenomena*, vol. 215, pp. 237–241, doi: [10.4028/www.scientific.net/SSP.215.237](https://doi.org/10.4028/www.scientific.net/SSP.215.237).